

Diffraction of 0.5 keV electrons from free-standing transmission gratings

Alex Cronin^a Ben McMorran^a T. A. Savas^b

^a*Department of Physics, University of Arizona
1118 E. 4th St, Tucson, AZ 85721*

^b*Department of Engineering, Massachusetts Institute of Technology
77 Massachusetts Ave, Cambridge, MA 92139*

Abstract

Diffraction of electrons with energy as low as 0.5 keV is demonstrated with a novel transmission grating in a scanning electron microscope. A 100-nm period grating with free-standing bars avoids the problem of inelastic scattering from the grating structure, and permits lower energy transmission electron diffraction than previously possible. Plans are presented to use similar gratings as coherent beam splitters for electron holography.

Key words: Low voltage electron diffraction, Electron holography, Electron interferometry, Inelastic scattering, Nanostructures, Nanofabrication.

PACS: 61.14

1 Introduction

Diffraction gratings for low energy electrons will open new frontiers in electron interferometry and holography. Until now, however, diffraction gratings have not been shown to transmit electrons with energy less than about 5 keV. This is because the standard diffraction grating for electrons is a thin slab of solid crystal, and inelastic scattering from the solid material destroys the diffraction pattern. Here we demonstrate a novel diffraction grating that works for much lower energy electrons. A nano-fabricated grating with free-standing bars was used to diffract 0.5 keV electrons. In this paper we first introduce some of the utility and difficulty associated with low energy transmission electron diffraction, then we describe the grating structures and techniques used here to observe electron diffraction. Finally, we propose some further experiments to study the de Broglie wave phase of the diffracted electron beams.

Interference fringes in an electron hologram contain information about a sample that is not available with standard electron microscope techniques. For example, electron holography (1; 2; 3; 4; 5) has been used to measure sample thickness, contact potentials, inner potentials, electric fields, and magnetic fields with nanometer resolution. According to the principle of electron holography, a beam splitter is required in order to create two separated paths for electron waves. Crystal diffraction gratings, apertures, or the small tip of a field emission gun can serve as beam splitters. However, certain advantages will be realized if a diffraction grating could be used as a beam splitter for low energy electrons. For example, good holograms can be made with a thermal filament electron gun if a diffraction grating is used (6) because the transverse coherence length of the electron waves is only required to be as large as the grating period (100 nm here). Using a thermal source brings the advantages of higher current and relaxed vacuum requirements. The low-energy limit is interesting because holographic measurements are more sensitive with lower energy electrons. Phase shifts due to a sample are large if low energy electrons are used, as illustrated by the equation

$$\phi = \frac{1}{\hbar} \sqrt{\frac{m_e}{2E}} \int_{\Gamma} U dx \quad (1)$$

where ϕ is the phase shift of an electron, \hbar is Planck's constant divided by 2π , m_e is the electron mass E is the electron energy, U is the interaction potential energy associated with a sample, and Γ is the classical path of the electron through the potential (4; 7). This motivates the search for an efficient diffraction grating for low energy electron waves.

Unfortunately, the standard techniques of electron diffraction from thin slabs of solid crystals work poorly for low energy electrons because of inelastic scattering. It has been shown that diffraction efficiency is optimized if the crystal thickness is similar to the inelastic mean free path of electrons. But, inelastic mean free path decreases with electron energy as shown in Table 1 (8; 9). Therefore the minimum thickness of an unsupported crystal slab sets a lower bound on the energy of electrons that can be diffracted. For 300 keV electrons, diffraction gratings made from thin foils of gold crystals approximately 60 nm thick already work as beam splitters for electron holograms (6). For diffraction of 5 keV electrons, crystal gratings less than 40 nm thick have been used (10; 11) simply to observe diffraction. No transmission diffraction gratings are readily available for electrons with energy lower than 5 keV.

To make progress in this area, we have used nanoscale gratings fabricated with free-standing bars separated by physical slots. This permits diffraction of electrons with energies as low as 0.5 keV. This is possible because electrons transmitted through the periodic slots have not passed close enough to the material walls to undergo inelastic scattering.

Table 1

Variation of inelastic mean free path with electron energy

Electron Energy	Inelastic Mean Free Path	Material	Reference
1000.0 keV	71.6 nm	Al	Mausawe 1981
100.0 keV	27.4 nm	Al	Mausawe 1981
2.0 keV	4.0 nm	Si	Tanuma 1991
0.5 keV	1.3 nm	Si	Tanuma 1991
0.1 keV	0.5 nm	Si	Tanuma 1991

To distinguish this work from established techniques of Low Energy Electron Diffraction (LEED) and Electron Back Scatter Diffraction (EBSD), let it be emphasized that LEED and EBSD work in reflection mode. In particular, LEED avoids the problem of inelastic scattering because it only depends on interactions in the first few nanometers of a sample. However, the reflection geometry in LEED and EBSD setups is not amenable to transmission holography arrangements proposed by Mertens (6), Missiroli (12) or Pozzi (13; 14). These holography techniques each require transmission diffraction gratings that work as coherent beam splitters.

2 Free-standing Gratings

The grating structures shown in Figs. 1 and 2 are made from silicon nitride material by T. A. Savas and H. I. Smith at the MIT NanoStructures laboratory. The free-standing 51-nm wide bars are separated by 49-nm wide slots, are 160 nm thick, and are slightly trapezoidal in cross section. The grating period of 100 nm is well defined by the fabrication process (15; 16). These transmission gratings have recently become important tools for atom optics and atom interferometry (17), in part because atoms interact strongly with matter. Hence it is natural to extend the use of these gratings to low energy electrons that also interact strongly with matter.

Because silicon nitride is an insulator, the gratings were sputter-coated with a 10-nm layer of Au/Pd and grounded to avoid charging. An attempt was made without the metal coating, but electron diffraction could not be observed. It was also found that the Au/Pd coating had to be reapplied after storing the gratings in air for one month. Apparently the Au/Pd coating becomes coated with organic contaminants over time.

To study electron diffraction, the 100-nm period Au/Pd-coated silicon nitride gratings were mounted in an Hitachi S-2460N scanning electron microscope (SEM) below the objective lens as shown in Fig. 3. The transmitted probe

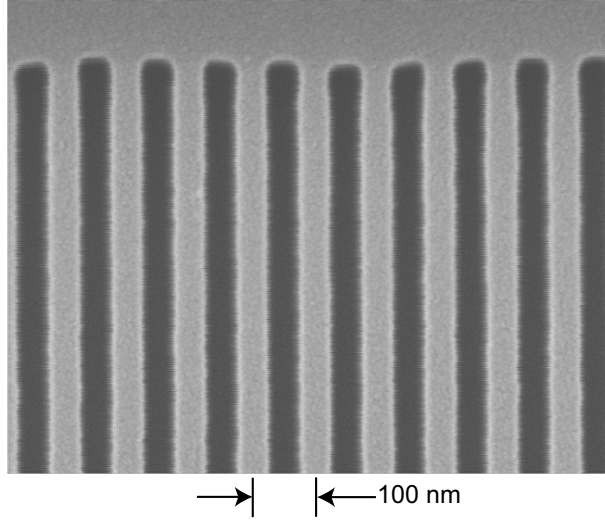


Fig. 1. An Au/Pd coated 100 nm period grating imaged with a Leo SEM using a 5 keV probe and 2 mm working distance. The dark regions are physical slots.

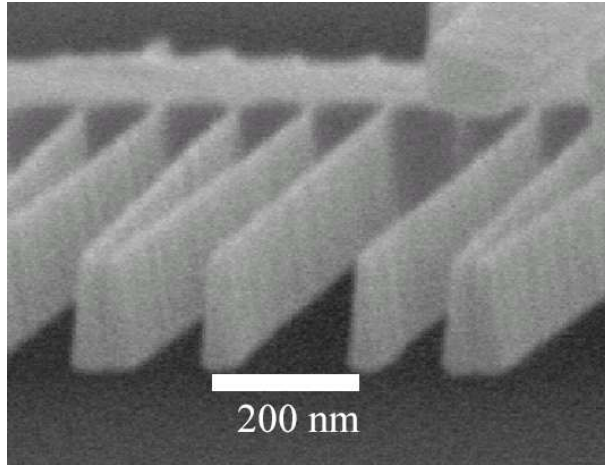


Fig. 2. An uncoated free-standing grating imaged with a Leo SEM using a 1.5 keV probe, and a 3 mm working distance. The sample is broken away from its support structure and tilted 80 degrees to view the cross-section of the grating bars.

was focused by the objective lens to a spot 32 mm below the grating. As a result of diffraction, the probe was found to be concentrated in multiple spots corresponding to the 1, 0 and -1 diffraction orders.

The multiple probe spots are separated by a distance s given in the small angle approximation by:

$$s = \frac{L\lambda_{dB}}{d_g} \quad (2)$$

In these experiments, $L = 32$ mm is the distance from the grating to the focused probe spots, λ_{dB} is the electron wavelength and $d_g = 100$ nm is the grating period. The electron wavelength is given by de Broglie's formula $\lambda_{dB} =$

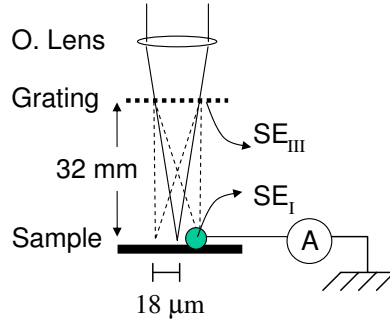


Fig. 3. Location of the objective lens, diffraction grating, and sample. The specimen current (A) and secondary electron (SE_I) signals are indicated. Secondary electrons generated at the grating (SE_{III}) produce a background signal.

h/p where h is Planck's constant and p is the electron momentum. The electron wavelength in Angstroms is $\lambda_{dB} = (150/V)^{1/2}$ where V is the accelerating potential in volts. Hence, for a 0.50 keV electron beam, $\lambda_{dB} = 0.55 \text{ \AA}$, and the diffracted probe spots are separated by $s = 18\mu\text{m}$.

3 Low Energy Electron Diffraction Results

The diffracted probe beam was studied using two techniques. First, the specimen current deposited on a $4\text{-}\mu\text{m}$ wire was measured while the diffracted probe was scanned across the wire. Next, scanning electron microscope (SEM) images were generated with the diffracted probe. The specimen current was measured with a picoamp meter and recorded with a computer. The $4\text{-}\mu\text{m}$ diameter tungsten wire was oriented parallel to the grating bars and the standard SEM scan mechanism was used to scan the probe perpendicular to the wire. Fig. 4 shows multiple peaks in the specimen current due to the resolved diffraction orders sequentially depositing electrons onto the wire. Second and third order diffraction peaks are faintly evident.

The SEM images shown in Fig. 5 are based on secondary electron (SE_I) signals generated with the same probe, grating and wire alignment. The SE_I signal strength as a function of probe position is extracted from the images by averaging the values of pixels in columns to plot a line profile for each image.

Additional SEM images with the grating in place show more evidence for diffraction. Figs. 6 and 7 show the secondary electron signal generated while scanning the diffracted probe over a wire screen sample located 22 mm below the grating. A stainless steel screen with $20\text{-}\mu\text{m}$ diameter wires was used as a sample because it has high secondary electron contrast and sharp edges in

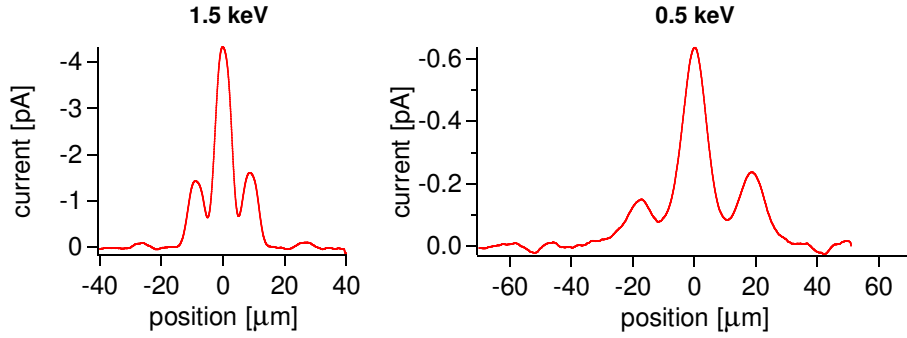


Fig. 4. Current deposited on a 4- μm diameter wire using electron beam energies of 1.5 keV (left) and 0.5 keV (right). The electron beam was diffracted as described in the text.

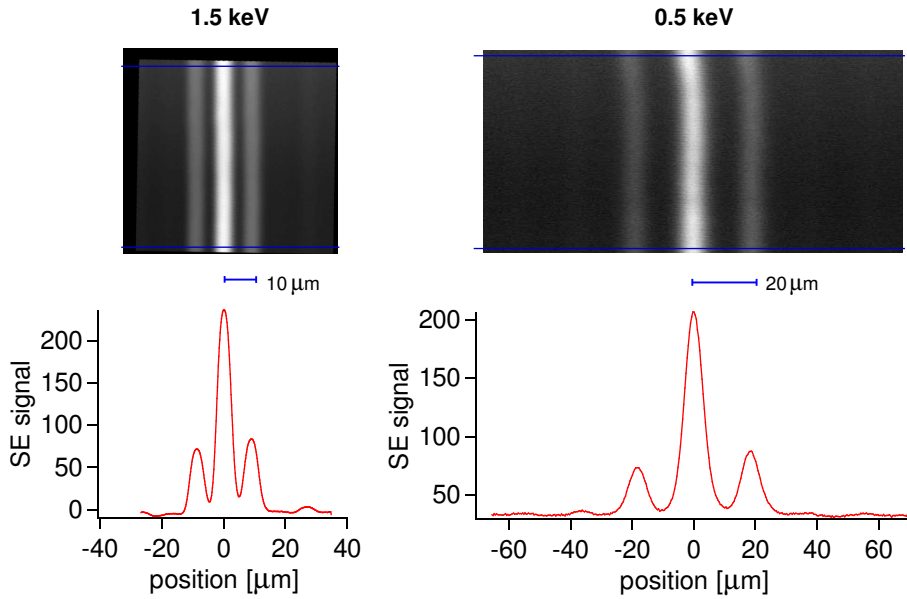


Fig. 5. (Top) SEM images of a single wire obtained with a diffracted electron beam probe. (Bottom) Line profiles of secondary electron signal were generated from the images.

two directions. The image appears in triplicate due to 1, 0, and -1 orders of the diffracted probe, and there is evidence for the weaker 2nd and 3rd orders. The probe is diffracted perpendicular to the grating bars, as expected from basic diffraction theory.

4 Further Experiments on Electron Coherence

While diffraction itself is a phenomenon that only applies to waves, we have not yet confirmed that electron waves in the different diffraction orders are

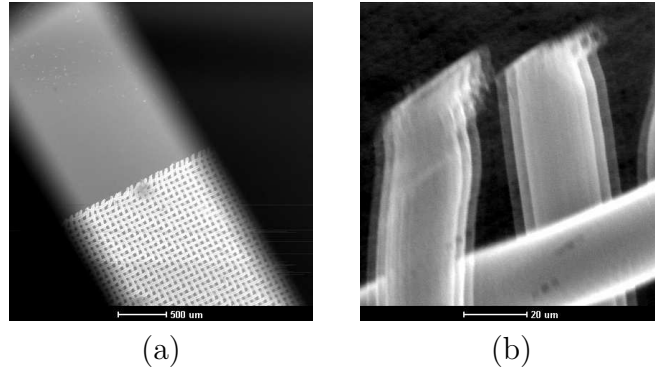


Fig. 6. SEM images of a 20- μm diameter wire mesh obtained with 6 keV electron beam that has passed through a diffraction grating. (a) With low magnification, the frame supporting the diffraction grating is visible. The 10,000 free-standing bars in the 1 mm aperture are not resolved because the electron beam is not focused on the grating, but on the mesh sample 22 mm below. (b) With higher magnification, an image of the wire mesh reveals ghost images because the electron beam has been diffracted. The orientation is the same for both images. The grating bars run parallel to the long axis of the aperture in (a). The ghost images in (b) are displaced along the perpendicular to the bars, as expected from diffraction theory.

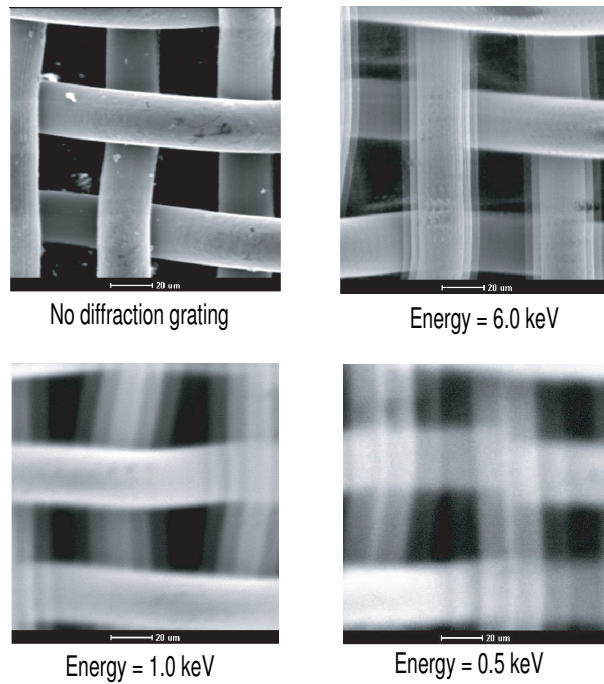


Fig. 7. Images of a 20- μm diameter wire mesh obtained in an SEM using a diffracted probe beams of different energy. Each image was taken at a magnification of 600x.v

sufficiently coherent to be used for interferometry. Inelastic interactions with the grating or fluctuating phase shifts may prevent an interferometer built with these gratings from showing any fringe contrast. To study the phase coherence of the diffracted electrons, we propose five experiments described below.

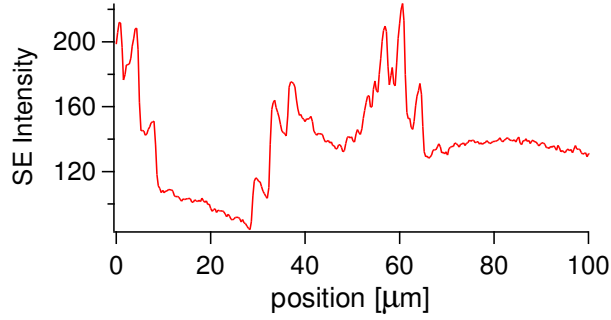


Fig. 8. Line profile from part of an image made with 6 kV accelerating voltage. Ten rows of the pixels were averaged to generate this plot. The separation between the peaks was measured to find the displacement between the diffracted probe spots.

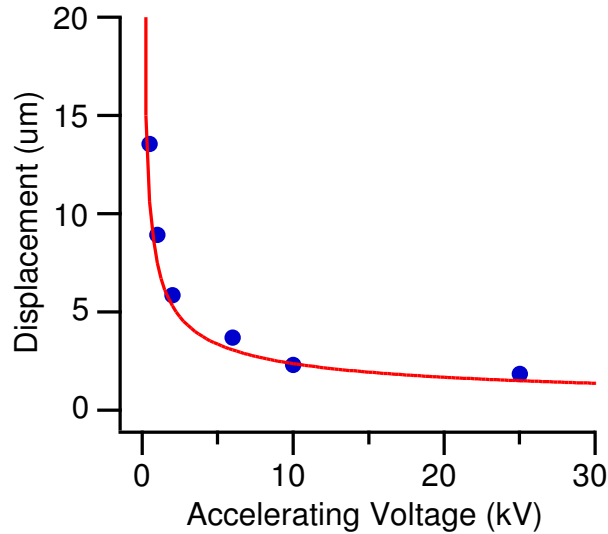


Fig. 9. Probe displacement depends on accelerating voltage. The theory (curve) has no adjustable parameters. It is entirely determined by Planck’s constant, the electron mass, the accelerating voltage, grating period, and grating-to-sample distance as given in Eq. 2. The data (dots) were obtained from SEM images as described in the text.

Electron waves should be slightly perturbed by image charges in the grating bars. Moving image charges that cause Joule heating have been proposed as a mechanism for decoherence (18). But the same image charges should also cause a coherent phase shift on the transmitted and diffracted electron waves that varies as a function of position within each slot. We have analyzed the position-dependent phase shift as a complex transmission function, and find that a coherent phase shift should cause changes in the relative current in each diffraction order as a function of electron energy. This experiment is similar in spirit to the measurement of atom-surface interactions accomplished with similar gratings by Grisenti (19; 20), and Perreault (21). Because the current in each diffraction order is expected to change most significantly for the second- and third-order diffraction peaks, the well-resolved patterns with a low background demonstrated in Fig. 4 look like a promising start for studying

this effect.

Another predicted effect due to coherent interactions between electrons and wedged grating bars is asymmetric diffraction patterns. Electron flux into each diffraction order should also change as a function of electron beam incidence angle on the grating. These are similar to atom optics investigations carried out by Cronin (22) to measure atom-surface van der Waals interactions. The first experiment of this sort for electrons was done recently by Herman Batelaan and coworkers at the University of Lincoln, Nebraska. Preliminary results suggest that a coherent phase shift for electrons is caused by transmission through the grating slots. Again, our data shown in Fig. 4 looks useful for studying this effect.

Irregular phase shifts caused by the grating should broaden the electron beam. Thus, we plan to study the width of the central diffraction peak as compared to the width of the raw electron beam generated without the grating. Our data in Figs. 4 and 7 show that the transmitted electron beam is broader at lower energies. However, this cannot yet be attributed to the grating. An exception is the case of non-metalized gratings, which were clearly observed to broaden the electron beam to the point where images of the steel mesh could not be produced with the transmitted beam.

Phase profiles could be engineered for the electron waves by applying an external electric field to polarize the bars of the grating. A related trick would be the application of a voltage gradient across the grating structure in an attempt to make an asymmetric "blazed" diffraction pattern.

To study electron wave coherence in near-field diffraction, one could search for the Talbot effect. The Talbot effect causes self-imaging of grating structures at multiples of the Talbot length, $z_T = d^2/\lambda_{dB}$, where λ_{dB} is the electron wavelength and d is the grating period (23; 24). Due to the Talbot effect, electron transmission through two gratings should oscillate as a function of the relative transverse position of the two gratings. This oscillation should have highest contrast if the gratings are separated longitudinally by multiples of 0.67 mm, which is the Talbot length for 6 keV electrons and grating structures with $d = 100$ nm. Related experiments, using atoms instead of electrons, were performed by Chapman (25) and Nowak (26). A requirement for seeing the Talbot effect is a beam divergence angle smaller than d/z_T , which is smaller than 150 microradians in this example. The Talbot effect, also known as Fourier self-imaging, should ideally make for perfect contrast in each Talbot image. Measurements of the Talbot image contrast would be a precise way to study the coherence of diffracted electron waves in the near field after a material diffraction grating.

The decisive experiment to verify that the diffracted beams are phase coherent

would be a working electron interferometer, using a geometry such as the one proposed by Marton (27; 28). The corresponding atom interferometer has already been built using free-standing gratings (29), and has been used for fundamental studies based on measurements of atom wave phase shifts. Until now, no similar device has been made for low energy electrons for lack of suitable diffraction gratings. An interferometer for low energy electrons would permit measurements of the index of refraction for electron waves due to dilute atomic and molecular gasses as proposed by Schmiedmayer (30), and could also be used to measure the gravitational mass of the electron as compared to the positron as discussed by Adelberger (31).

A hybrid grating-and-biprism interferometer is another method to explore the coherence in diffracted electron beams. An electron holography instrument as originally proposed by Gabor (1) could be modified to incorporate one diffraction grating and one biprism as suggested by Mertens (6), Missiroli (12) or Pozzi (13; 14). These instruments were originally conceived for use with a crystal beam splitter, and we now propose to replace the solid crystal with fabricated periodic structures. Such an experiment may be the easiest way to verify the phase coherence of the diffracted probe beams and pioneer the frontier of low-energy electron holography.

5 Summary

In conclusion, the problem of inelastic scattering in transmission electron diffraction has been largely avoided by using a new kind of diffraction grating for electrons. Instead of diffraction from a solid crystal lattice, a fabricated structure with free-standing physical bars allows diffraction to be observed with low energy (0.5 keV) electrons. This is transmission electron diffraction at ten times lower energy than any previously reported (10), and should enable new research in electron optics.

6 Acknowledgements

This research was supported by an Award from Research Corporation, NSF grant ECS-0404350, and NSF grant PHY-0354947.

References

- [1] D. Gabor, Microscopy by reconstructed wavefronts, *Proceedings of the Royal Society of London. Series A: Mathematical and physical sciences* 197 (1051) (1949) 454.
- [2] A. Tonomura, Applications of electron holography, *Review of Modern Physics* 59 (3) (1987) 639.
- [3] A. Tonomura, Present and future of electron holography, *Journal of Electron Microscopy* 38 (1989) S43.
- [4] A. Tonomura (Ed.), *International Workshop on Electron Holography*, Elsevier, Amsterdam, 1994.
- [5] A. Tonomura, *Electron Holography*, Springer, Berlin, 1999.
- [6] B. Mertens, M. Overwijk, P. Kruit, Off-axis holography with a crystal beam splitter, *Ultramicroscopy* 77 (1999) 1–11.
- [7] C. Cohen-Tannoudji, B. Diu, F. Laloe, *Quantum Mechanics*, J. Wiley and Sons, 1977.
- [8] R. Al-Mausawe, T. Quinn, The effect of amorphous material on the contrast of electron diffraction patterns, *Journal of Physics D: Applied physics* 15 (1982) 267–274.
- [9] D. Penn, Electron mean-free-path calculations using a model dielectric function, *Physical Review B* 35 (2) (1987) 482–486, see also: http://xdb.lbl.gov/Section3/Sec_3-2.html.
- [10] E. Shizgal, personal communication (2004).
- [11] L. Drummy, J. Yang, D. Martin, Low-voltage electron microscopy of polymer and organic molecular thin films, *Ultramicroscopy* 99 (2004) 247.
- [12] G. Missiroli, G. Pozzi, U. Valdr, Electron interferometry and interference electron microscopy, *Journal of Physics E* 14 (1981) 649–671.
- [13] G. Pozzi, Off-axis image electron holography proposal, *Optik* 47 (1977) 105.
- [14] G. Pozzi, Off-axis image electron holography with a mixed type interferometer, *Optik* 63 (1983) 227.
- [15] T. Savas, S. Shah, M. Schattenburg, J. Carter, H. Smith, Achromatic interferometric lithography for 100-nm-period gratings and grids, *Journal of Vacuum Science and Technology B* 13 (6) (1995) 2732–2735.
- [16] T. Savas, M. Schattenburg, J. Carter, H. Smith, Large-area achromatic interferometric lithography for 100 nm period gratings and grids, *Journal of Vacuum Science and Technology B* 14 (6) (1996) 4167–4170.
- [17] P. Berman (Ed.), *Atom Interferometry*, Academic Press, San Diego, 1997.
- [18] J. Anglin, W. Zurek, A precision test of decoherence, [quant-ph/9611049](http://arxiv.org/abs/quant-ph/9611049) v2.
- [19] R. Grisenti, W. Schollkopf, J. Toennies, G. Hergerfeldt, T. Kohler, Determination of atom-surface van der Waals potentials from transmission-grating diffraction intensities, *Physical Review Letters* 83 (9) (1999) 1755–1758.
- [20] R. Grisenti, W. Schollkopf, J. Toennies, J. Manson, T. Savas, H. Smith,

- He-atom diffraction from nanostructure transmission gratings: The role of imperfections, *Physical Review A* 61 (2000) 033608.
- [21] J. Perreault, A. Cronin, T. Savas, Using atomic diffraction of Na from material gratings to measure atom-surface interactions, arXiv:physics/0312123 To appear in *Phys. Rev. A*.
- [22] A. Cronin, J. Perreault, Phasor analysis of atom diffraction from a rotated material grating, *Physical Review A* 70 (4) (2004) 043607.
- [23] R. Leggat, Talbot, William Henry Fox, <http://www.rleggat.com/photohistory/history/talbot.htm> (2000).
- [24] M. Berry, I. Marzoli, W. Schleich, Quantum carpets, carpets of light, <http://physicsweb.org/article/world/14/6/7> (2001).
- [25] M. Chapman, C. Ekstrom, T. Hammond, J. Schmiedmayer, B. Tannian, S. Wehinger, D. Pritchard, Near-field imaging of atom diffraction gratings: The atomic Talbot effect, *Physical Review A* 51 (1) (1995) R14–R17.
- [26] S. Nowak, C. Kurtsiefer, T. Pfau, C. David, High-order Talbot fringes for atomic matter waves, *Optics Letters* 22 (18) (1997) 1430–1432.
- [27] L. Marton, Electron interferometer, *Physical Review* 85 (1952) 1057–1058.
- [28] L. Marton, H. Suddeth, An electron interferometer, *Review of Scientific Instruments* 25 (1954) 1099.
- [29] D. Keith, C. Ekstrom, Q. Turchette, D. Pritchard, An interferometer for atoms, *Physical Review Letters* 66 (21) (1991) 2693–2697.
- [30] R. Forrey, A. Dalgarno, J. Schmiedmayer, Determining the electron forward-scattering amplitude using electron interferometry, *Physical Review A* 59 (1999) R942.
- [31] E. Adelberger, B. Heckel, C. Stubbs, Y. Su, Does antimatter fall with the same acceleration as ordinary matter?, *Physical Review Letters* 66 (7) (1991) 850–853, time cited: 26.